AQUEOUS FOAMS IN THE PRESENCE OF SURFACTANT CRYSTALS

Bernard P. Binks* and Hui Shi

Department of Chemistry and Biochemistry, University of Hull, Hull. HU6 7RX. UK

Submitted to: Langmuir on 16.12.19; revised 14.1.20

Contains ESI

*Correspondence to: b.p.binks@hull.ac.uk

Keywords: Aqueous foam; surfactant crystals; particle-stabilized foam

ABSTRACT

Aqueous foams are used extensively in many fields and anionic surfactants are commonly used foaming agents. However, potential trouble may arise when they are utilized in hard water areas and/or at low temperatures. Anionic surfactants, like sodium dodecyl sulfate (SDS), may precipitate in the form of crystals when the concentration of divalent counterions such as Mg^{2+} exceeds a certain limit. In an attempt to prepare ultra-stable foams containing precipitated crystals, the behaviour of SDS in water was systematically investigated as a function of surfactant concentration at different concentrations of $Mg(NO_3)_2$ prior to a study of their foam properties. We quantitatively study the conversion of surfactant micelles to crystals and the re-dissolution of crystals into micelles. It was found that the presence of surfactant crystals reduced the initial foam volume and foam half-life but greatly improved the long-term stability of foams. Foam studies were also conducted for the supernatant and sediment isolated from crystal dispersions so that the importance of surfactant crystals to foam stability could be established. Despite the foamability of a sediment being low, an order of magnitude increase in foam half-life was related to the coverage of bubble surfaces by surfactant crystals. Both rapid cooling and ultrasonication were shown to influence the surfactant crystal shape and size with an impact on foam properties.

INTRODUCTION

An aqueous foam is a dispersion of gas bubbles in water and anionic surfactants such as sodium dodecyl sulfate (SDS) are the most commonly used foaming agents.[1-4] Surfactant-stabilized aqueous foams are common and products are extensively used in many fields like food, pharmaceuticals, cleaning and cosmetics.[5-11] As is well-known, foams stabilized by surfactants are thermodynamically unstable and destabilization occurs through a combination of drainage, coalescence and disproportionation.[12-16] Unlike surfactants, solid particles with appropriate wettability can possess much higher adsorption energy to the air-water interface and give rise to foams of long-term stability.[17,18] More and more studies have focused on particle-stabilised foams in the last decade or so.[19-22] Binks and co-workers carried out a series of studies with silane-grafted fumed silica particles of varying hydrophobicity and aqueous foams generated were completely stable against coalescence.[23-25] Alargova *et al.*[26] and Liu *et al.*[27] produced foams stabilised by synthetic polymer microrods or plate-like layered double hydroxide particles respectively. Foam bubbles were sterically separated by a dense layer(s) of interfacial particles endowing the foam with high stability.

In the literature, examples exist in which particles are elaborately synthesized or modified *ex situ*.[28,29] Only a few articles report aqueous foams stabilised by solid surfactant particles. Shrestha *et al.* used dilute aqueous dispersions of pentaglycerol monostearate ($C_{18}G_5$) to form highly persistent foams at 25 °C.[30,31] In the presence of finely dispersed small surfactant solid particles, an increased surface viscosity played a role in enhancing foam stability. More recently, Zhang *et al.* reported on ultra-stable aqueous foams by precipitating surfactant *in situ* on air bubble surfaces.[32,33] Upon adding NaCl or KCl to aqueous SDS solutions, surfactant crystals form during foam generation. At intermediate salt concentrations, foams undergo disproportionation and drainage is reduced as crystals block the Plateau borders. At high salt concentrations, foams do not coarsen or drain and crystals become close packed on bubble surfaces. Ionic surfactants are likely to precipitate in the form of crystals due to a decreased solubility below the Krafft point.[34,35] For anionic surfactants in particular, conditions leading to surfactant precipitation are easy to meet in conditions of low temperature or hard water. However, the stabilization of aqueous foams in the presence of surfactant crystals has not received much attention.

We have carried out a systematic study to link the process of surfactant precipitation to foaming performance. According to the precipitation domain of magnesium dodecyl sulfate (in excess of either of the precipitation components $Mg(NO_3)_2$ or SDS),[36] quantitative studies

concerning the conversion of surfactant molecules from monomers to micelles and/or crystals have been conducted along with simultaneous foam studies to assess their impact on foaming ability and foam stability. Compared to the work of Zhang *et al.*,[32,33] we have investigated over forty different concentrations for surfactant and divalent salt which cut through different regions in the phase diagram and where surfactant crystals are formed before foaming. In addition to conventional characterization of the foams, foam studies of the supernatant and sediment isolated from crystal dispersions also helped us understand the separate roles of surfactant crystals and free surfactant molecules to long-term foam stability. Finally, rapid cooling and ultrasonication of aqueous phases were found to greatly influence the shape and size of surfactant crystals formed which further impacts on foam properties.

EXPERIMENTAL

(a) Materials

Anionic surfactant sodium dodecyl sulfate (SDS, > 99%), magnesium nitrate hexahydrate ($Mg(NO_3)_2 \cdot 6H_2O$, > 99%), cationic surfactant Hyamine 1622 (≥ 99%), disulphine blue VN (dye content ≥ 40%) and dimidium bromide (≥ 95%) were purchased from Sigma-Aldrich and used as received. Sulphuric acid (≥ 95%) and chloroform (≥ 99.8%) were purchased from Fisher Chemical and also used as received. Water was purified by passing through an Elgastat Prima reverse osmosis unit followed by a Millipore Milli-Q reagent water system. It had a surface tension of 72.0 mN m^{-1} at 25 °C measured with a Krüss K11 tensiometer and a du Noüy ring.

(b) Methods

All experiments were conducted at room temperature (T = 20 ± 3 °C) except for those involving rapid cooling. [SDS] and [$Mg(NO_3)_2$] represent the initial concentration of SDS and $Mg(NO_3)_2$ in the system respectively (mM).

Preparation of surfactant solutions/crystal dispersions. Aqueous SDS solutions were prepared at varying SDS concentrations with and without 10 mM $Mg(NO_3)_2$. The concentration of SDS ranged from 0.1 mM to 200 mM. Also, aqueous SDS solutions of 0.5 mM and 15 mM were prepared at varying $Mg(NO_3)_2$ concentrations. The concentration of $Mg(NO_3)_2$ varied from 0.1 mM to 100 mM. Surfactant precipitated as crystals forming crystal dispersions in some of these mixtures (see Table S1).

Determination of actual surfactant concentration in supernatant and sediment. Each crystal dispersion separated into a supernatant and sediment after standing for 2 days. The volume fraction of supernatant (ϕ_{sup}) and sediment (ϕ_{sed}) was determined from height measurements (see Figure S1). The equilibrium concentration of free surfactant in the supernatant was determined using the two-phase Epton titration involving Hyamine 1622 as a cationic titrant.[37] 1 mL of supernatant was pipetted into a 100 mL stoppered mixing cylinder. 2 mL of aqueous indicator solution containing 0.14 mM disulphine blue, 0.21 mM dimidium bromide and 0.1 mM sulphuric acid was then added followed by 10 mL of Milli-Q water and 15 mL of chloroform. An aqueous solution of 1.009 mM Hyamine 1622 was then added as titrant from a burette. As titration proceeded, there was a colour change until it reached the end-point when the pink colour in the chloroform layer turned grey-blue and the yellow colour in the water layer turned green (see Figure S2). Each titration was repeated three times to determine the average. The concentration of surfactant within a sediment was calculated applying a mass balance (see ESI) and three samples were also titrated to verify these calculations.

Crystal size measurement. The particle size of surfactant crystals was measured using a Malvern Mastersizer 2000 equipped with a Hydro 2000SM dispersion unit. 1 mL of crystal dispersion was dispersed in 120 mL of aqueous $Mg(NO_3)_2$ solution of the corresponding concentration and stirred at a speed of 1000 rpm. Each measurement was set to repeat three times and three parallel measurements were carried out to take the average. This measurement based on light scattering provides us with a volume-equivalent spherical diameter for the crystals. However, optical microscopy of surfactant crystal length with ImageJ software analysis revealed very little difference in the sizes obtained.

Foam generation. 20 mL of each SDS solution or crystal dispersion was transferred to a 250 mL (max. 320 mL) glass graduated cylinder and sealed with a leak-proof stopper. An aqueous foam was generated by shaking the graduated cylinder by hand vigorously for 15 sec (about 60 up-down cycles) – a protocol we have found reproducible in previous studies. The volume of foam produced and the volume of drained liquid were immediately recorded after shaking and as a function of time. The foamability and foam stability are characterized by the initial foam volume (V_{f0}) and foam half-life ($t_{1/2}$) respectively. Each solution/crystal dispersion was repeatedly foamed by the same operator three times to determine the average values of V_{f0} and $t_{1/2}$. The possibility exists that surfactant crystals are reduced in size during foaming.

Microscopy. Surfactant crystals and foam bubbles were observed immediately after preparation using an Olympus BX51 optical microscope. Micrographs were taken with a 16-bit Olympus

DP70 camera with Image Pro Plus software. By using a U-POT polarizer and a reflected light analyser (U-AN, Olympus T2 Japan), crossed-polarized light was also applied for these observations. Additionally, cryo-scanning electron microscopy (SEM) was carried out on a fresh foam formed from a sediment separated from a crystal dispersion of 30 mM SDS in 10 mM $Mg(NO_3)_2$ (see ESI.)

Rapid cooling and ultrasonication. Crystal dispersions of 2-30 mM SDS in 10 mM $Mg(NO_3)_2$ were held in a 60 ℃ water bath (IKA RCT basic) for 2 h and then moved to a 0 ℃ water bath (Grant Optima™ TC120) directly. They cooled down from 60 ℃ to 11 ℃ within 4 min while stirring with a glass rod. Surfactant precipitated as crystals during this rapid cooling process (14 ℃ min^{-1}). These crystal dispersions showed no sign of subsequent precipitation or re-dissolution after storing at room temperature (T = 20 ± 3 ℃) for 5 h and foam studies were conducted using 500 mL (max. 650 mL) glass graduated cylinders. Additionally, four samples of 30 mM SDS in 10 mM $Mg(NO_3)_2$ crystal dispersions were freshly prepared at room temperature and treated using a high-intensity ultrasonic processor (100 Watt, Sonic & Materials VC100 Vibra-cell) equipped with a CV18 ultrasonic probe (tip diameter: 3 mm). Crystal dispersions were sonicated at an amplitude of 100% for different times (1-10 min) in a 20 ℃ water bath. Foams were then formed in 500 mL (max. 650 mL) glass graduated cylinders at room temperature (T = 20 ± 3 ℃).

RESULTS AND DISCUSSION

(a) Precipitation of SDS upon adding $Mg(NO_3)_2$

It is known that the presence of $Mg(NO_3)_2$ brings different effects to aqueous SDS solutions depending on the concentration of both SDS and $Mg(NO_3)_2$. The most common phenomenon is that an increase in salt concentration decreases the critical micelle concentration (*cmc*). This is a result of the charge neutralization of surfactant head groups by counterions facilitating micellization.[38] The *cmc* values of SDS at [$Mg(NO_3)_2$] of 0 mM, 1 mM, 10 mM and 100 mM were determined by surface tension and experimental details are described in the ESI. Above the *cmc* a solid surfactant phase may form. It is affected by the interactions between the cations of the electrolyte and micelles whereby ion exchange induces the precipitation of $Mg(DS)_2$ given its higher Krafft point (T_k = 25 ℃) compared to SDS in pure water (T_k = 15 ℃).[39,40] The precipitation domain of $Mg(DS)_2$ at 20 ℃ was reported by Kallay *et al.*[36] which we redraw alongwith our determined *cmc* values in Figure 1. Herein, we have

studied four types of concentration variation which cut through different regions, denoted as arrowed lines 1-4 in Figure 1.

As expected, aqueous SDS solutions with no $Mg(NO_3)_2$ added are all clear solutions between 0.1 mM and 200 mM surfactant (arrow 1). As the *cmc* of SDS in pure water is about 8 mM (cmc_0 = 8 mM, subscript refers to salt concentration in mM), surfactant exists as monomer below it and in the form of micelles above it. While the *cmc* of SDS decreases to approximately 1 mM (cmc_{10} = 1 mM) in the presence of 10 mM $Mg(NO_3)_2$ (arrow 2), additional surfactant molecules precipitate instead of forming micelles between around 2 mM and 30 mM surfactant, as seen in Figure 2(a). Above this range, re-dissolution of precipitated crystals occurs as a result of a considerable increase in micelle concentration inducing a strong ion-micelle interaction and a decreased Mg^{2+} ion activity coefficient.[41] In the case of fixing the surfactant concentration at 0.5 mM, we vary the [$Mg(NO_3)_2$] from 0.1 mM to 100 mM (arrow 3). Since 0.5 mM SDS is lower than the *cmc* values over the whole salt concentration range, only clear monomer solutions form. At an [SDS] of 15 mM which is above all the *cmc* values however (arrow 4), clear micellar solutions exist at low salt concentrations whereas surfactant precipitation occurs upon increasing [$Mg(NO_3)_2$] to 3 mM and above (Figure 2(b)). We note that there is a slight upward shift of the upper boundary of the precipitation domain compared to the reported one.[36] We believe that the difference lies in the purities of surfactant and salt used over 30 years ago and now.

A crystal dispersion of 8 mM SDS in 10 mM $Mg(NO_3)_2$ and an aqueous solution of 10 mM $Mg(NO_3)_2$ were observed in crossed-polarized light inside a dark box (see Figure S3). The crystal dispersion appears much brighter than the homogeneous and isotropic salt solution as seen in Figure 2(c). Precipitated crystals are anisotropic such that crossed-polarized light is rotated through the sample. Additionally, optical microscope images of surfactant crystals are given in Figure 2(d) and Figures S4 and S5. It can be seen that crystals are irregularly plate-like (of thickness few μm) and polydisperse in size from tens of microns to several hundred microns. The average diameter of surfactant crystals measured using light diffraction varies little upon increasing the surfactant concentration (≈ 150 μm, Figure S6) but decreases from around 180 μm to 80 μm with increasing salt concentration (Figure S7). The latter agrees with that reported by Li *et al.*[42] on the effect of $Mg(SO_4)_2$ concentration on the crystallization of calcium oxalate. Raising the salt concentration led to a reduction in both the nucleation and growth rate of crystals.

(b) Conversion of surfactant monomers to micelles and crystals

The appearance of crystal dispersions of 2-30 mM SDS in 10 mM $Mg(NO_3)_2$ after standing for two days is given in Figure 3(a-1) and that of crystal dispersions of 15 mM SDS in 3-100 mM $Mg(NO_3)_2$ is given in Figure 3(b-1) respectively. The concentration of surfactant in supernatants ($[SDS]_{actual,sup}$) and in sediments ($[SDS]_{actual,sed}$) was obtained as described earlier, as well as the number of moles of surfactant taking into account their volumes (calculation given in ESI). They are plotted in Figure 3(a-2), (a-3), (b-2) and (b-3). The nature of surfactant molecules in supernatants was determined by comparing $[SDS]_{actual,sup}$ with *cmc* values.

In the presence of 10 mM $Mg(NO_3)_2$, we can see from Figure 3(a-2) and (a-3) that surfactant molecules preferentially precipitate into crystals within the range of [SDS] = 2 - 15 mM while the monomer concentration in the supernatant remains constant close to the *cmc*. When $c_{actual,sed}$ reaches a critical value upon increasing [SDS] to 20 mM, additional surfactant molecules no longer precipitate into crystals but accumulate in the supernatant in the form of micelles. At a fixed [SDS] of 15 mM, Figure 3(b-2) and (b-3) reveal that over two-thirds of surfactant exists as monomers and micelles in the supernatant with the remaining one third being within the sediment at a salt concentration of 3 mM. Upon increasing the salt concentration up to 10 mM, the continual conversion of surfactant molecules to surfactant crystals occurs. When $[SDS]_{actual,sup}$ is lowered to the *cmc* value (cmc_{10} = 1 mM), $n_{actual,sup}$ and $n_{actual,sed}$ remain constant thereafter up to a salt concentration of 100 mM.

Overall, there is a distribution equilibrium between surfactant as monomers, micelles and crystals: surfactant micelles start to form only when crystals have reached saturation and there are excess surfactant molecules. This quantitative study of surfactant distribution in supernatants and sediments separated from crystal dispersions is necessary to understand the results of their foaming performance.

(c) Foam behaviour of surfactant solutions and crystal dispersions

We quantify the foamability of a liquid by its initial foam volume (V_{f0}) and the foam stability is discussed in terms of foam half-life ($t_{1/2}$, the time taken for a foam column to collapse to half its initial volume) and relative foam volume after 2 days. Foam studies were conducted for the four series of surfactant solutions and crystal dispersions shown in Figure 1.

In the case of 10 mM $Mg(NO_3)_2$ and increasing surfactant concentration (arrow 2 in Figure 1), variation of V_{f0} and $t_{1/2}$ with [SDS] are plotted in Figures 4 and 5 respectively with insets illustrating the form of surfactant which prevails. The foamability increases up to the *cmc* of 1 mM after which it decreases once crystals begin to form. In the precipitation range, V_{f0} increases only slightly but increases dramatically once micelles form in surfactant crystal dispersions (between 15 mM and 40 mM SDS). At 50 mM SDS and above, all surfactant crystals re-dissolve into molecules and V_{f0} is restored to values exhibited by micellar solutions in the absence of salt. For comparison, for SDS solutions in the absence of $Mg(NO_3)_2$ (arrow 1 in Figure 1), V_{f0} increases progressively with increasing surfactant concentration up to 30 mM and then decreases slightly by 200 mM, as shown with a dashed line in Figure 4. The reduction in V_{f0} at high [SDS] is thought to be due to an increase in micelle life-time which delays the replenishment of surfactant monomers to the fresh bubble surfaces.[43,44] It is clear from the data that crystal dispersions (with salt) are much less foamable than surfactant solutions (without salt) between 2 mM and 20 mM SDS. This is in line with reports that particle dispersions do not produce much foam.[33] By considering dynamic surface tensions of a range of surfactants forming dilute lamellar phases, Garrett and Gratton[45] argued that the slow transport of surfactant from 'particles' of lamellar phase to the air-water surface does not involve breakdown to monomers but by a combination of the emergence of 'particles' into the surface followed by spreading. The latter spreading may not occur however for surfactant crystals. Bubbles in foams generated from monomer solutions up to 1 mM SDS are spherical and have smooth surfaces (Figure 6). In foams generated from crystal dispersions at [SDS] between 2 and 40 mM, surfactant crystals compete with molecular surfactant for bubble surfaces and crystals partition between the surface and bulk. At and above 50 mM SDS where only micelles exist, bubbles possess smooth surfaces again.

Regarding foam stability, without salt, $t_{1/2}$ increases dramatically up to the *cmc* (8 mM) but decreases progressively beyond it. The former is due to the increased monomer concentration on bubble surfaces inducing increased repulsion between adsorbed surfactant layers retarding bubble coalescence. The latter may arise from the stepwise layer-by-layer thinning of micelles within foam films and the restricted volume effect in the film.[46-48] With salt, the half-life $t_{1/2}$ is very low for SDS concentrations yielding monomers or monomers + crystals but increases to around 500 min as micelles form in the presence of crystals and remains relatively high as crystals re-dissolve. In comparison to the corresponding SDS solutions without salt, foam stability is dramatically decreased in the presence of salt over the

range where surfactant crystals appear ([SDS] = 2-30 mM). This is mainly due to the reduction in the concentration of molecular surfactant by crystal formation. If sufficient surfactant crystals adsorbed to bubble surfaces during foaming, one would expect an increased foam stability compared with those containing molecular surfactant alone. Our findings suggest that a certain proportion of surfactant crystals remain in water (see Figure 6) and could potentially pierce aqueous foam films contributing to enhanced instability. At relatively high surfactant concentrations where surfactant molecules exist as monomers + micelles ([SDS] = 50-200 mM), foam half-life is only slightly lower in the presence of salt because Mg^{2+} can screen the electrostatic repulsion of dense surfactant layers between two air-water interfaces and subsequently cause thinning and rupture of foam films.[49,50]

A similar scenario occurs in the series at a fixed SDS concentration of 15 mM with increasing salt concentration (arrow 4 in Figure 1). Before the majority of surfactant precipitates into crystals, the foamability is not significantly affected below 2 mM $Mg(NO_3)_2$ (see Figure S8). Once surfactant crystals are formed, V_{f0} decreases sharply and reaches a low plateau value above *ca*. 20 mM salt when no micelles remain. This demonstrates that the presence of micelles which deliver surfactant monomers is more favourable for foaming compared with that of surfactant crystals as the latter diffuse slower to bubble surfaces. Moreover, $t_{1/2}$ is reduced over the whole range of [$Mg(NO_3)_2$] compared to a 15 mM SDS micellar solution with no salt added, particularly in the presence of crystals but absent of micelles (see Figure S9). As mentioned above, Mg^{2+} ions can compress the electrical double layer on bubble surfaces leading to reduced repulsion between bubbles. Microscopy of foams shown in Figure 7 reveals smooth, spherical bubbles from micellar solutions (1 mM salt) and crystal-containing dispersions with a high concentration of micelles (3 mM salt). However, once all micelles are used up (≥ 10 mM salt), surfactant crystals partially coat air bubbles endowing them with textured surfaces as in particle-stabilised foams. The surface of a single bubble at 50 mM salt is not fully covered by crystals however, the bare areas containing surfactant monomer. This allows bubbles to coarsen which, as suggested in ref. 33, may induce desorption of crystals as they rearrange and eventual foam collapse.

Finally, at a fixed SDS concentration of 0.5 mM which is below the *cmc* for all salt concentrations and where only monomers exist (arrow 3 in Figure 1), V_{f0} is little affected by salt concentration (Figure S10) whereas $t_{1/2}$ (which is low throughout) passes through a small maximum at 1 mM $Mg(NO_3)_2$ (Figure S11). As discussed by Angarska *et al*.[51] for SDS foam films and foams, addition of divalent counterions like Mg^{2+} can influence foam film/foam

stability in opposing directions. The surface elasticity and viscosity may increase due to the bridging of adjacent surfactant headgroups by magnesium ions (stabilising) or there may be an enhancement of the ionic correlation attraction between film surfaces due to ion adsorption in the Stern layer (destabilising). Both effects are dependent on the concentrations of electrolyte and surfactant.

As mentioned earlier, particle-stabilised foams generally possess superior stability to surfactant-stabilised ones.[26,33] However, this advantage is not apparent here in the data for foams containing surfactant crystals if we only use $t_{1/2}$ to describe foam stability. Instead, we quantify the long-term stability of foams by determining the ratio of the residual foam volume after two days to the initial foam volume (V_{f2d}/V_{f0}). Figure 8 shows the variation of V_{f2d}/V_{f0} for series 2 and 4 which involve surfactant crystal formation. Foams formed from dispersions containing an adequate amount of crystals are more stable in the long-term than micellar solutions despite the higher surfactant concentration required for the latter. We monitored the appearance of bubbles at the top and towards the bottom of the foam column as it drained for a surfactant crystal+micelle dispersion (Figure S12). Bubbles remain spherical in the lower layer but become non-spherical and polyhedral in the upper layer. Even after 1 min the surfaces of these bubbles appear structured and it is likely that surfactant crystals are adsorbed at least partially. A proportion may also remain in the thin aqueous films between bubbles as the foam becomes dry.

(d) Comparison of supernatants, sediments and crystal dispersions

To further understand the roles of free surfactant and surfactant crystals in foam behaviour, clear supernatants and crystal-concentrated sediments were separated from crystal dispersions after standing for two days. Foam studies were carried out for supernatants and sediments in the same way as above and compared to those of intact crystal dispersions. Figures 9 and 10 show the variations of V_{f0} and $t_{1/2}$ as a function of actual surfactant concentration for the same volume of the three kinds of aqueous phase (series 2). Regarding the foamability, generating the same volume of foam requires the highest surfactant concentration for sediments followed by crystal dispersions and lowest for supernatants. The sequence of foamability is thus supernatant > crystal dispersion > sediment. Furthermore, we used the initial foam volume of supernatants ($V_{f0,sup}$) and sediments ($V_{f0,sed}$) and their volume fractions in crystal dispersions (ϕ_{sup} and ϕ_{sed}) to derive the initial foam volume of intact crystal dispersions using

$$V_{f0,calculated} = \phi_{sup} \cdot V_{f0,sup} + \phi_{sed} \cdot V_{f0,sed} \quad (1)$$

The derived initial foam volume ($V_{f0,calculated}$) is plotted as a dashed line in Figure 9 where it can be seen to be very close to the experimental data. This demonstrates that free surfactant (mainly in supernatants) and surfactant crystals (mainly in sediments) both contribute in a superimposed way to the foamability of intact crystal dispersions.

By comparing surfactant concentrations needed to achieve a certain $t_{1/2}$ for foams formed from supernatants, sediments and crystal dispersions, the order of foam stability is sediment > supernatant > crystal dispersion. In addition, $t_{1/2}$ of foams from sediments is over an order of magnitude higher than that for both supernatants and intact crystal dispersions and the former display excellent long-term stability (see Table 1). In series 2, values of V_{f2d}/V_{f0} for supernatant foams are either zero (complete foam collapse) or very low as a function of SDS concentration. Those for sediment foams however increase from 0.2 to between 0.5 and 0.6 in the same range. Intact crystal dispersions exhibit long-term stability between the two. In series 4, all supernatant foams collapsed completely within two days and values of V_{f2d}/V_{f0} for intact crystal dispersions fluctuates around 0.15. Although the destabilizing effect of salt is observed at high salt concentrations, V_{f2d}/V_{f0} for sediment foams is significantly high (0.5-0.7) at low salt concentrations.

Since a sediment is concentrated in surfactant crystals, it is predicted that the enhanced stability of foams prepared from them is due to the increased coverage of bubbles by surface-active surfactant crystals. To prove this, foams formed from crystal dispersions and sediments were observed using crossed-polarizers as shown in Figure 11(a-c). Foams produced from intact crystal dispersions give perfectly spherical bubbles with smooth surfaces with few crystals adsorbed. However, bubbles in foams from sediments are rougher and brighter indicating higher surfactant crystal coverage. Cryo-SEM images given in Figure 11(d) confirm the plate-like morphology of crystals and compactly covered bubble surfaces. A high surface density of adsorbed crystals can retard bubble coalescence and inter-bubble gas transfer leading to the outstanding stability of foams from sediments. This is in line with reports on ultra-stable foams in which an armoured layer of solid particles imparts excellent stability to both spherical and non-spherical bubbles.[25,52,53] The same conclusions were drawn from foam studies in series 4 for 15 mM SDS as a function of salt concentration (Figures S13-S16).

(e) Ultrasonication and rapid cooling

Since the precipitation of surfactant crystals at room temperature has limited control of both the size and shape of crystals, ultrasonication and rapid cooling were used separately to

effect changes in the morphology of crystals. By applying energy to break surfactant crystals prepared at room temperature, ultrasonication was employed to reduce the crystal size. The average diameter of surfactant crystals within 30 mM SDS in 10 mM $Mg(NO_3)_2$ crystal dispersions decreases with increasing time of ultrasonication, as shown in Figure 12(a). The decrease is from around 150 μm without sonication to 45 μm, 29 μm, 21 μm and 17 μm after sonicating for 1 min, 2 min, 5 min and 10 min respectively (Figure S17). The impact of crystal size reduction on foam properties was investigated. As shown in Figure 12(b), both V_{f0} and $t_{1/2}$ display a maximum as a function of average crystal diameter. The foamability and foam stability initially increase on decreasing the crystal diameter, probably as a result of an increase in the number concentration of crystals. The decrease in both parameters for smaller crystals cannot be explained at present.

Rapid cooling is an alternative way to control crystal size/morphology. While preparing crystal dispersions of SDS in 10 mM $Mg(NO_3)_2$, rapid cooling renders crystals more uniform and square in shape, as shown in microscope images of Figure 13(a). The average crystal diameter decreases to between 85 μm and 110 μm compared with those prepared at room temperature (145 μm-175 μm, Figure S18). Such a change however has virtually no impact on foam properties of crystal dispersions, as shown in Figure 13(b).

CONCLUSIONS

In the presence of magnesium nitrate, aqueous solutions of SDS at room temperature form plate-like surfactant crystals in equilibrium with surfactant monomers and micelles. Once formed, crystal dispersions exhibit lower foamability than either monomeric or micellar solutions at the same surfactant concentration. The foamability of a crystal dispersion containing dissolved surfactant molecules can be calculated from the respective foamabilities of the separate phases knowing their volume fractions. Surfactant crystals partition between bulk water and air bubble surfaces. If crystal adsorption is low however, disproportionation and coalescence occur through surfactant molecule-coated areas leading to foam collapse. If crystals close-pack on bubble surfaces, foams stable in the long-term can be prepared. Ultrasonication of crystal dispersions results in a decrease in the size of surfactant crystals and both foamability and foam stability are optimised for crystals of intermediate size.

ACKNOWLEDGMENTS

The authors thank the University of Hull for a PhD Scholarship to HS and Mr. A. Sinclair (University of Hull) for carrying out the cryo-SEM measurements.

REFERENCES

(1) Bikerman, J.J. in *Foams*; Springer-Verlag, Berlin, 1973.

(2) Prud'homme, R.K.; Khan., S.A. in *Foams: Theory, Measurements and Applications*; Marcel Dekker, Inc., New York, 1995.

(3) Pugh, R.J. in *Bubble and Foam Chemistry*; Cambridge University Press, Cambridge, 2016.

(4) Schramm, L.L. in *Emulsions, Foams, and Suspensions: Fundamentals and Applications*; Wiley-VCH, Weinheim, 2005.

(5) Acharya, D.P.; Gutiérrez, J.M.; Aramaki, K.; Aratani, K.; Kunieda, H. Interfacial Properties and Foam Stability Effect of Novel Gemini-Type Surfactants in Aqueous Solutions. *J. Colloid Interface Sci.* **2005**, *291*, 236-243.

(6) Koczó, K.; Rácz, G. Foaming Properties of Surfactant Solutions. *Colloids Surf.* **1991**, *56*, 59-82.

(7) Goff, H.D. Formation and Stabilisation of Structure in Ice-Cream and Related Products. *Curr. Opin. Colloid Interface Sci.* **2002**, *7*, 432-437.

(8) Wu, C.; Wang, Z.Y.; Zhi, Z.Z.; Jiang, T.Y.; Zhang, J.H.; Wang, S.L. Development of Biodegradable Porous Starch Foam for Improving Oral Delivery of Poorly Water Soluble Drugs. *Int. J. Pharm.* **2011**, *403*, 162-169.

(9) Broze, G. in *Handbook of Detergents: Properties*; Marcel Dekker, Inc., New York, 1999.

(10) Baki, G.; Alexander, K.S. in *Introduction to Cosmetic Formulation and Technology*; John Wiley & Sons, Hoboken, 2015.

(11) Hill, C.; Eastoe, J. Foams: From Nature to Industry. *Adv. Colloid Interface Sci.* **2017**, *247*, 496-513.

(12) Koehler, S.A.; Hilgenfeldt, S.; Weeks, E.R.; Stone, H.A.; Foam Drainage on the Microscale II. Imaging Flow through Single Plateau Borders. *J. Colloid Interface Sci.* **2004**, *276*, 439-449.

(13) Wang, J.L.; Nguyen, A.V.; Farrokhpay, S. A Critical Review of the Growth, Drainage and Collapse of Foams. *Adv. Colloid Interface Sci.* **2016**, *228*, 55-70.

(14) Langevin, D. Bubble Coalescence in Pure Liquids and in Surfactant Solutions. *Curr. Opin. Colloid Interface Sci.* **2015**, *20*, 92-97.

(15) Bhakta, A.; Ruckenstein, E. Decay of Standing Foams: Drainage, Coalescence and Collapse. *Adv. Colloid Interface Sci.* **1997**, *70*, 1-124.

(16) Briceño-Ahumada, Z.; Langevin, D. On the Influence of Surfactant on the Coarsening of Aqueous Foams. *Adv. Colloid Interface Sci.* **2017**, *244*, 124-131.

(17) Binks, B.P.; Horozov, T.S. in *Colloidal Particles at Liquid Interfaces*; Cambridge University Press, Cambridge, 2006.

(18) Binks, B.P.; Horozov, T.S. Aqueous Foams Stabilized Solely by Silica Nanoparticles. *Angew. Chem. Int. Ed.* **2005**, *44*, 3722-3725.

(19) Gonzenbach, U.T.; Studart, A.R.; Tervoort, E.; Gauckler, L.J. Ultrastable Particle-Stabilized Foams. *Angew. Chem. Int. Ed.* **2006**, *45*, 3526-3530.

(20) Binks, B.P.; Rocher, A. Stabilisation of Liquid-Air Surfaces by Particles of Low Surface Energy. *Phys. Chem. Chem. Phys.* **2010**, *12*, 9169-9171.

(21) Binks, B.P. Particles as Surfactants – Similarities and Differences. *Curr. Opin. Colloid Interface Sci.* **2002**, *7*, 21-41.

(22) Horozov, T.S. Foams and Foam Films Stabilised by Solid Particles. *Curr. Opin. Colloid Interface Sci.* **2008**, *13*, 134-140.

(23) Binks, B.P.; Duncumb, B.; Murakami, R. Effect of pH and Salt Concentration on the Phase Inversion of Particle-Stabilized Foams. *Langmuir* **2007**, *23*, 9143-9146.

(24) Stocco, A.; Rio, E.; Binks, B.P.; Langevin, D. Aqueous Foams Stabilized Solely by Particles. *Soft Matter* **2011**, *7*, 1260-1267.

(25) Cervantes Martinez, A.; Rio, E.; Delon, G.; Saint-Jalmes, A.; Langevin, D.; Binks, B.P. On the Origin of the Remarkable Stability of Aqueous Foams Stabilised by Nanoparticles: Link with Microscopic Surface Properties. *Soft Matter* **2008**, *4*, 1531-1535.

(26) Alargova, R.G.; Warhadpande, D.S.; Paunov, V.N.; Velev, O.D. Foam Superstabilization by Polymer Microrods. *Langmuir* **2004**, *20*, 10371-10374.

(27) Liu, Q.; Luan, L.Y.; Sun, D.J.; Xu, J. Aqueous Foam Stabilized by Plate-Like Particles in the Presence of Sodium Butyrate. *J. Colloid Interface Sci.* **2010**, *343*, 87-93.

(28) Du, Z.P.; Bilbao-Montoya, M.P.; Binks, B.P.; Dickinson, E.; Ettelaie, R.; Murray, B.S. Outstanding Stability of Particle-Stabilized Bubbles. *Langmuir* **2003**, *19*, 3106-3108.

(29) Fujii, S.; Nakamura, Y. Stimuli-Responsive Bubbles and Foams Stabilized with Solid Particles. *Langmuir* **2017**, *33*, 7365-7379.

(30) Shrestha, L.K.; Acharya, D.P.; Sharma, S.C.; Aramaki, K.; Asaoka, H.; Ihara, K.; Tsunehiro, T.; Kunieda, H. Aqueous Foam Stabilized by Dispersed Surfactant Solid and Lamellar Liquid Crystalline Phase. *J. Colloid Interface Sci.* **2006**, *301*, 274-281.

(31) Shrestha, L.K.; Saito, E.; Shrestha, R.G.; Kato, H.; Takase, Y.; Aramaki, K. Foam Stabilized by Dispersed Surfactant Solid and Lamellar Liquid Crystal in Aqueous Systems of Diglycerol Fatty Acid Esters. *Colloids Surf. A* **2007**, *293*, 262-271.

(32) Zhang, L.; Mikhailovskaya, A.; Yazhgur, P.; Muller, F.; Cousin, F.; Langevin, D.; Wang, N.; Salonen, A. Precipitating Sodium Dodecyl Sulfate to Create Ultrastable and Stimulable Foams. *Angew. Chem. Int. Ed.* **2015**, *54*, 9533-9536.

(33) Zhang, L.; Tian, L.; Du, H.; Rouzière, S.; Wang, N.; Salonen, A. Foams Stabilized by Surfactant Precipitates: Criteria for Ultrastability. *Langmuir* **2017**, *33*, 7306-7311.

(34) Shinoda, K.; Yamaguchi, N.; Carlsson, A. Physical Meaning of the Krafft Point: Observation of Melting Phenomenon of Hydrated Solid Surfactant at the Krafft Point. *J. Phys. Chem.* **1989**, *93*, 7216-7218.

(35) Kunieda, H.; Shinoda, K. Krafft Points, Critical Micelle Concentrations, Surface Tension, and Solubilizing Power of Aqueous Solutions of Fluorinated Surfactants. *J. Phys. Chem.* 1976, *80*, 2468-2470.

(36) Kallay, N.; Pastuovic, M.; Matijević, E. Solubility and Enthalpy of Precipitation of Magnesium, Calcium, Strontium, and Barium Dodecyl Sulfates. *J. Colloid Interface Sci.* **1985**, *106*, 452-458.

(37) Reid, V.W.; Longman, G.F.; Heinerth, E. Determination of Anionic Detergents by Two-Phase Titration. *Tenside* **1967**, *4*, 292-304.

(38) Kumar, B.; Tikariha, D.; Ghosh, K.K. Effects of Electrolytes on Micellar and Surface Properties of Some Monomeric Surfactants. *J. Disp. Sci. Technol.* **2012**, *33*, 265-271.

(39) Miyamoto, S. The Effect of Metallic Ions on Surface Chemical Phenomena. III. Solubility of Various Metal Dodecyl Sulfates in Water. *Bull. Chem. Soc. Jpn.* **1960**, *33*, 371-375.

(40) Vautier-Giongo, C.; Bales, B.L. Estimate of the Ionization Degree of Ionic Micelles Based on Krafft Temperature Measurements. *J. Phys. Chem. B* **2003**, *107*, 5398-5403.

(41) Chou, C.I.; Bae, J.H. Surfactant Precipitation and Redissolution in Brine. *J. Colloid Interface Sci.* **1983**, *96*, 192-203.

(42) Li, M.K.; Blacklock, N.J.; Garside, J. Effects of magnesium on calcium oxalate crystallization. *J. Urol*. **1985**, *133*, 123-126.

(43) Oh, S.G.; Shah, D.O. The Effect of Micellar Lifetime on the Rate of Solubilization and Detergency in Sodium Dodecyl Sulfate Solutions. *J. Am. Oil Chem. Soc.* **1993**, *70*, 673-678.

(44) Binks, B.P.; Johnson, A.J.; Rodrigues, J.A. Inversion of 'Dry Water' to Aqueous Foam on Addition of Surfactant. *Soft Matter* **2010**, *6*, 126-135.

(45) Garrett, P.R.; Gratton, P.L. Dynamic surface tensions, foam and the transition from micellar solution to lamellar phase dispersion. *Colloids Surf. A* **1995**, *103*, 127-145.

(46) Saint-Jalmes, A.; Peugeot, M.L.; Ferraz, H.; Langevin, D. Differences between Protein and Surfactant Foams: Microscopic Properties, Stability and Coarsening. *Colloids Surf. A* **2005**, *263*, 219-225.
(47) Nikolov, A.D.; Wasan, D.T. Order Micelle Structuring in Thin Films Formed from Anionic Surfactant Solutions. *J. Colloid Interface Sci.* **1989**, *133*, 1-12.
(48) Laheja, A.P.; Basak, S.; Patil, R.M.; Khilar, K.C. Experimental Observations on Drainage of Foams Generated Using Micellar Solutions of Anionic, Cationic, and Nonionic Surfactants. *Langmuir* ***1998***, *14*, 560-564.
(49) Li, C.; Somasundaran, P. Role of Electrical Double Layer Forces and Hydrophobicity in Coal Flotation in Sodium Chloride Solutions. *Energy Fuels* **1993**, *7*, 244-248.
(50) Powale, R.S.; Bhagwat, S.S. Influence of Electrolytes on Foaming of Sodium Lauryl Sulfate. *J. Disp. Sci. Technol.* **2006**, *27*, 1181-1186.
(51) Angarska, J.K.; Tachev, K.D.; Kralchevsky, P.A.; Mehreteab, A.; Broze, G. Effects of Counterions and Co-ions on the Drainage and Stability of Liquid Films and Foams. *J. Colloid Interface Sci.* **1998**, *200*, 31-45.
(52) Subramaniam, A.B.; Abkarian, M.; Mahadevan, L.; Stone, H.A. Colloid Science: Non-Spherical Bubbles. *Nature* **2005**, *438*, 930-930.
(53) Binks, B.P.; Campbell, S.; Mashinchi, S.; Piatko, M.P. Dispersion Behavior and Aqueous Foams in Mixtures of A Vesicle-Forming Surfactant and Edible Nanoparticles. *Langmuir* **2015**, *31*, 2967-2978.

Table 1. Volume ratio of foam after 2 days to that just after preparation (V_{f2d}/V_{f0}) for varying SDS or $Mg(NO_3)_2$ concentrations prepared from either supernatants, intact crystal dispersions or sediments.

Varying SDS in 10 mM $Mg(NO_3)_2$ (series 2)	Form of surfactant		crystals + monomers				crystals + micelles		
	[SDS]/mM		2	5	8	15	20	25	30
	supernatant	V_{f2d}/V_{f0}	0	0	0	0	0	0.10	0.13
	crystal dispersion	V_{f2d}/V_{f0}	0	0	0.02	0.08	0.16	0.16	0.16
	sediment	V_{f2d}/V_{f0}	0.16	0.16	0.20	0.32	0.60	0.47	0.45
Varying $Mg(NO_3)_2$ in 15 mM SDS (series 4)	Form of surfactant		crystals + monomers				crystals + micelles		
	$[Mg(NO_3)_2]$/mM		3	5	7	10	30	50	100
	supernatant	V_{f2d}/V_{f0}	0	0	0	0	0	0	0
	crystal dispersion	V_{f2d}/V_{f0}	0	0.15	0.12	0.09	0.14	0.18	0.16
	sediment	V_{f2d}/V_{f0}	0.47	0.61	0.72	0.62	0.11	0.15	0.15

Figure 1. Precipitation domain of magnesium dodecyl sulphate $Mg(DS)_2$ in water at 20 °C. Solid precipitates form within the shaded region. Filled points are re-plotted from ref. 35. Red arrows 1-4 indicate the series of mixtures in which either [SDS] or $[Mg(NO_3)_2]$ varies. The *cmc* values were determined here by surface tension.

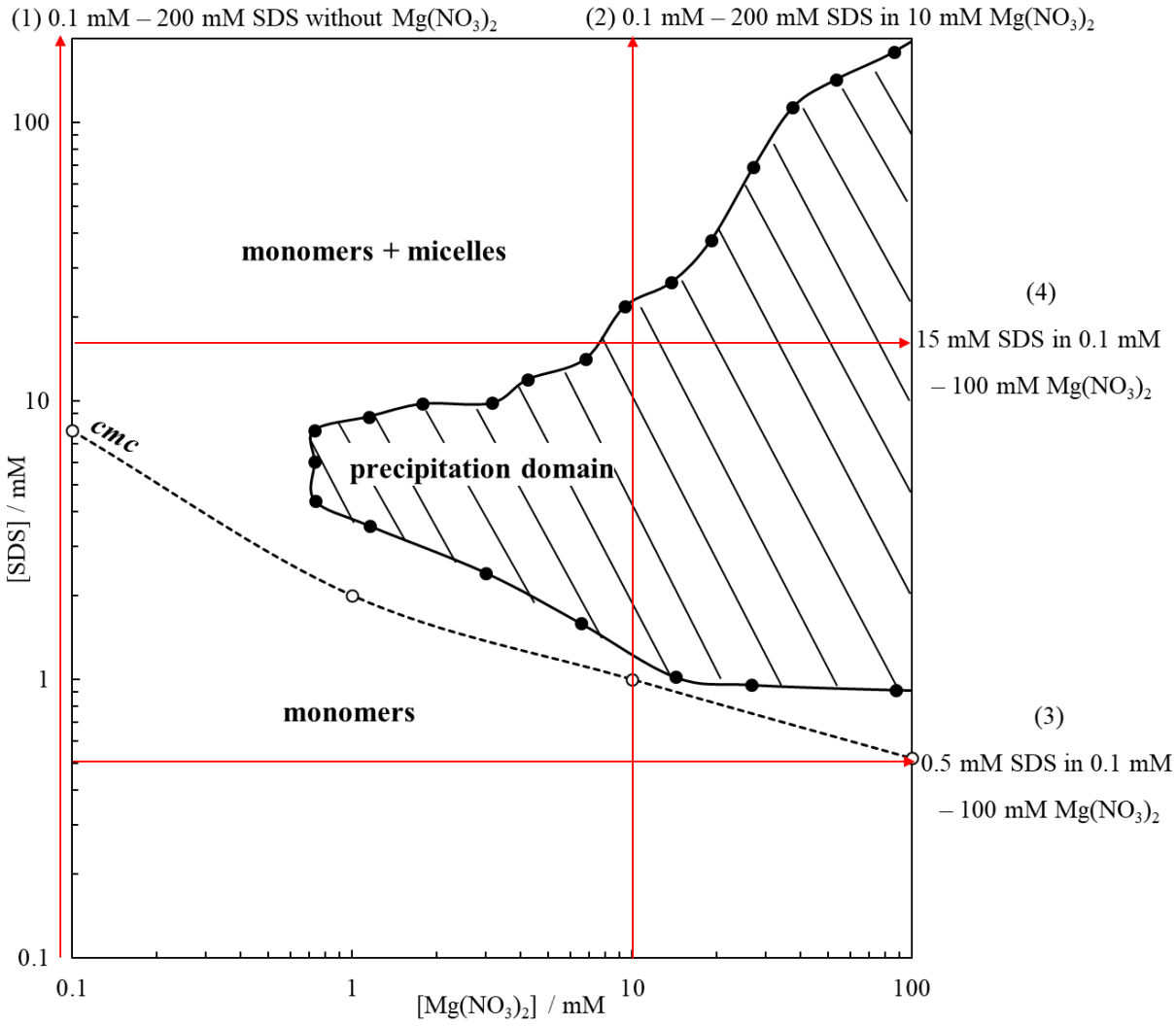

Figure 2. Photos of vessels containing (a) 10 mM $Mg(NO_3)_2$ at various [SDS] and (b) 15 mM SDS at various [$Mg(NO_3)_2$] after preparation at 20 ± 3 °C. Precipitation of surfactant crystals occurs within the red dashed frame. (c) Photos under cross-polarisers of (left) an isotropic aqueous solution of 10 mM $Mg(NO_3)_2$ and (right) an anisotropic surfactant crystal dispersion of 8 mM SDS in 10 mM $Mg(NO_3)_2$. (d) Optical microscope image of surfactant crystals (anisotropic irregularly-shaped flakes) in dispersion of 8 mM SDS in 10 mM $Mg(NO_3)_2$.

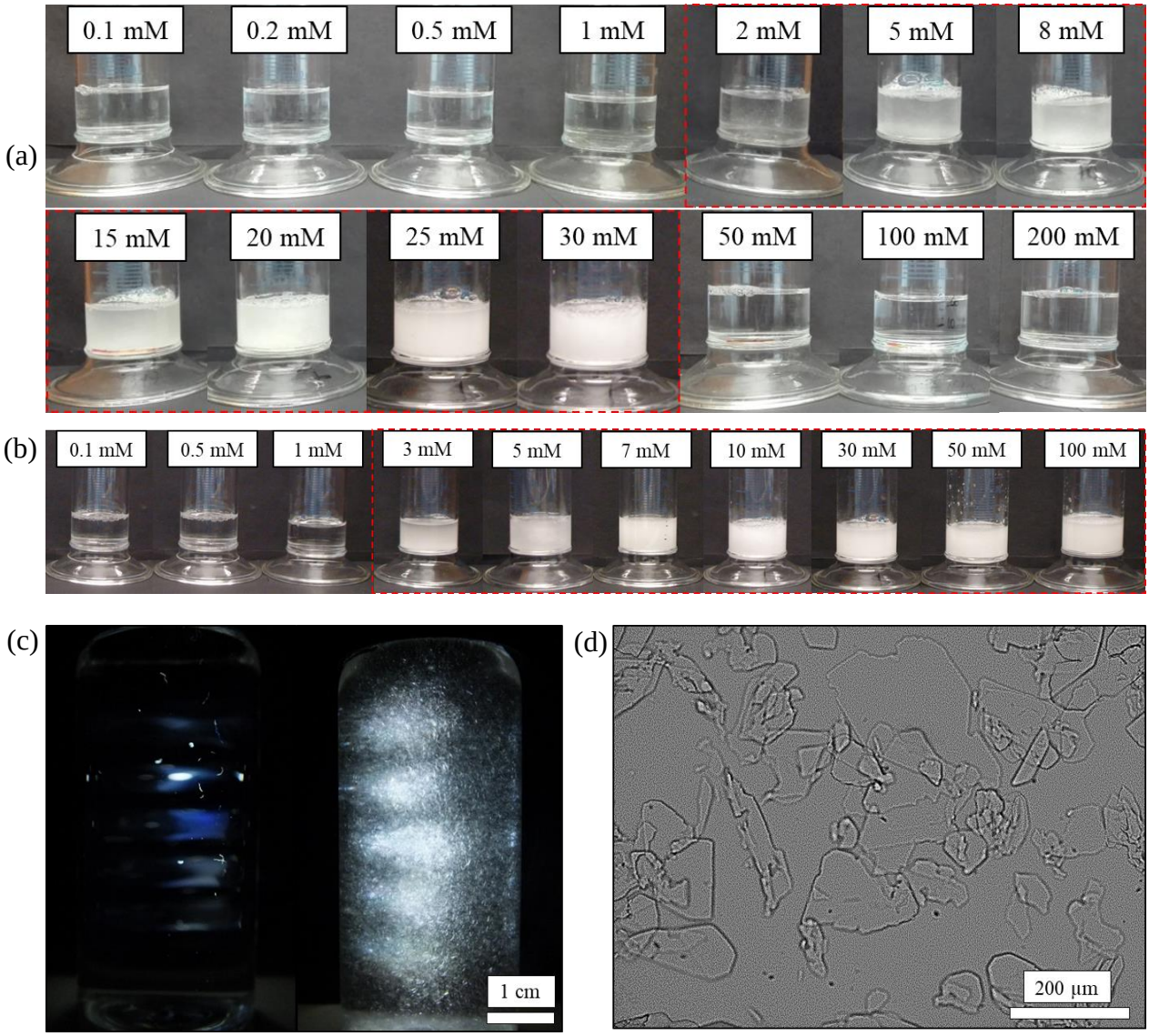

Figure 3. (a1) Photos of vessels containing crystal dispersions for various [SDS] in 10 mM $Mg(NO_3)_2$ after standing for 2 days. Variation of (a2) number of moles and (a3) concentration of surfactant in both supernatant and sediment separated from above dispersions *versus* [SDS]. Similarly, photos and surfactant variations of crystal dispersions for various [$Mg(NO_3)_2$] in 15 mM SDS are given in (b1)-(b3).

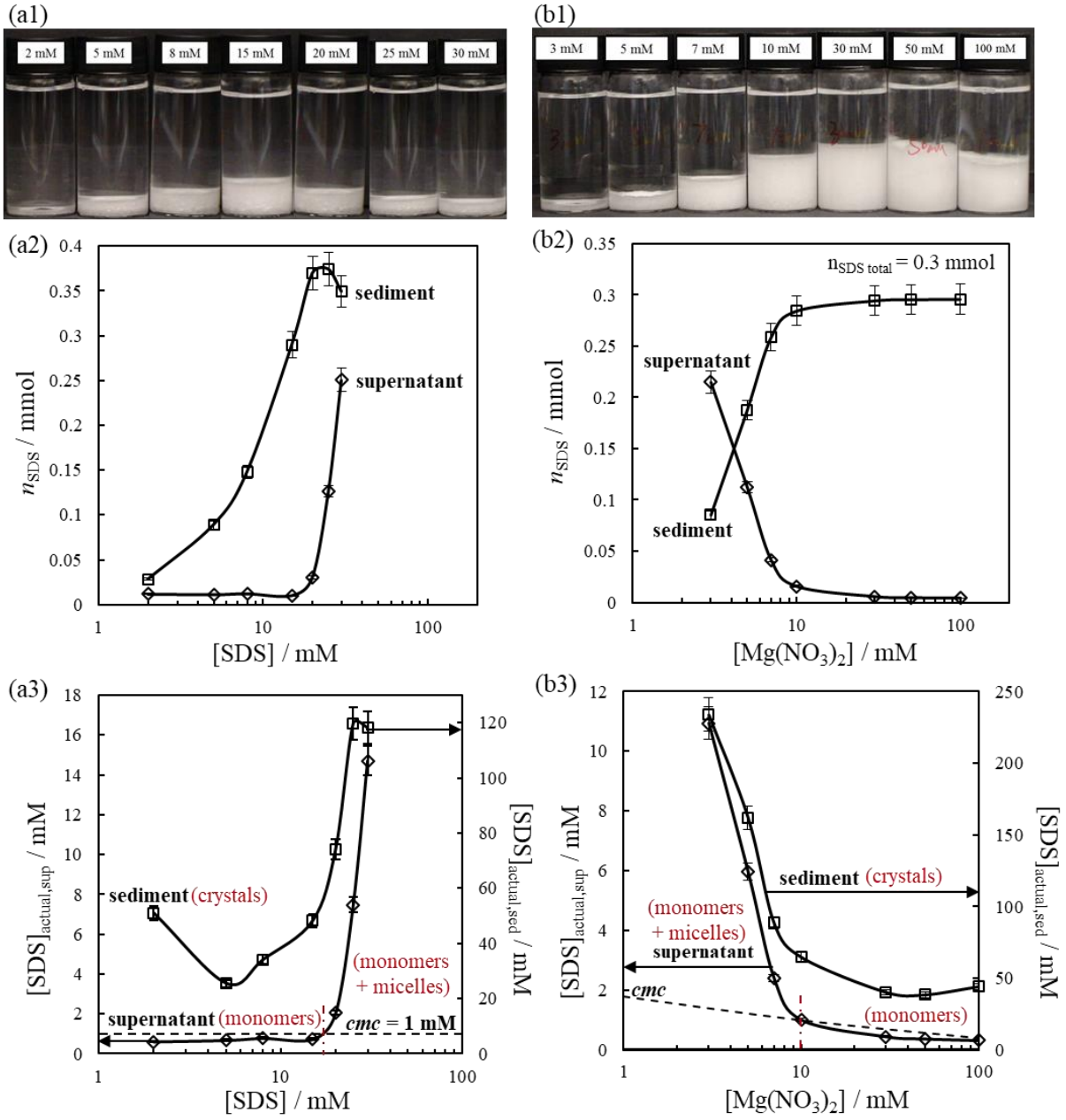

Figure 4. Variation of initial foam volume (V_{f0}) generated from 20 mL of aqueous SDS in 10 mM $Mg(NO_3)_2$ at 20 ± 3 °C as a function of [SDS] (filled points). Inset shows graduated cylinders containing these foams and red dashed frame denotes foams generated from crystal dispersions. For comparison, data for foams formed from aqueous SDS in pure water is also shown (open points).

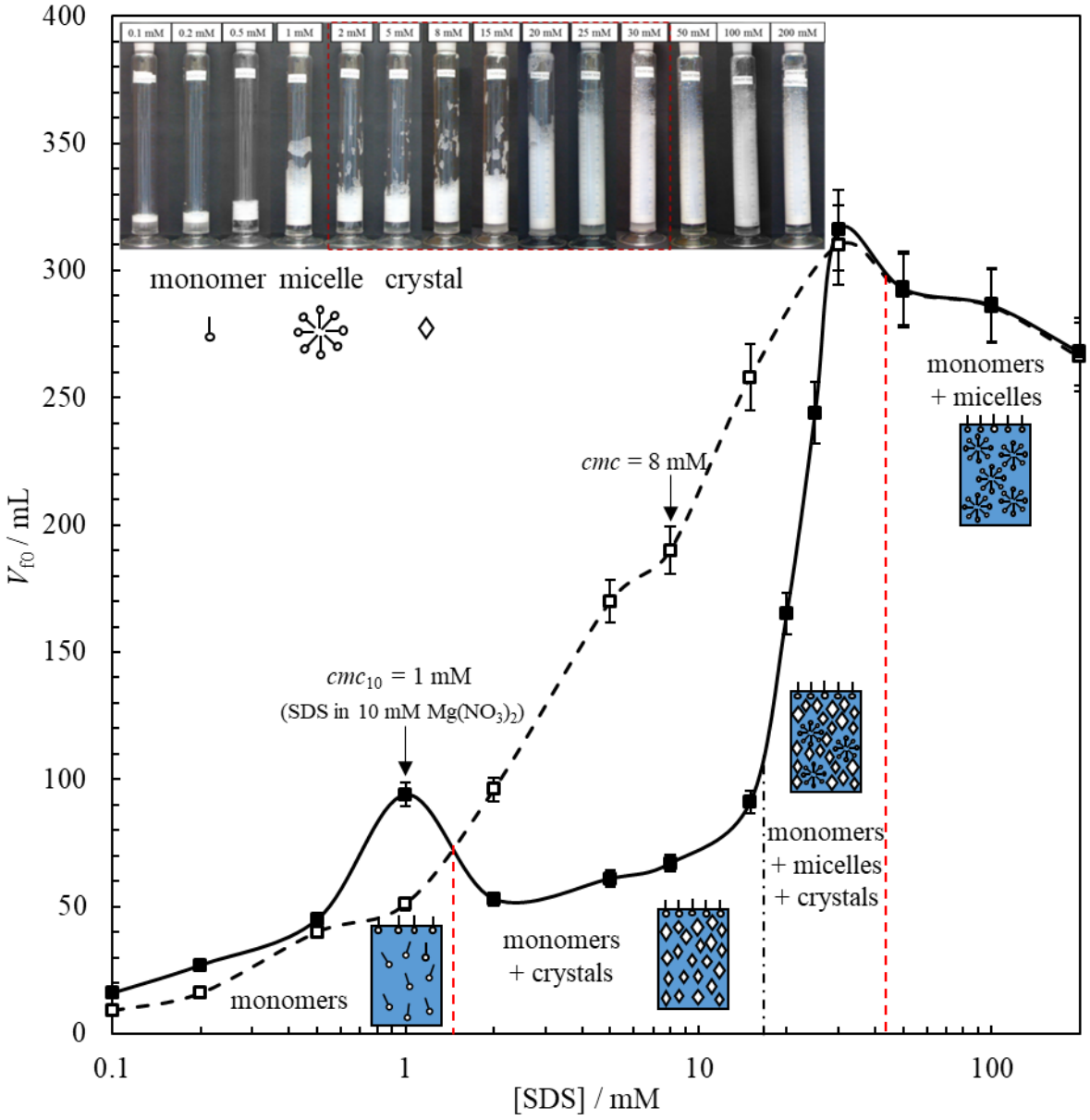

Figure 5. Variation of foam half-life ($t_{1/2}$) of aqueous foams generated from 20 mL of SDS in 10 mM $Mg(NO_3)_2$ at 20 ± 3 ℃ as a function of [SDS] (filled points). For comparison, data for foams formed from aqueous SDS in pure water is also shown (open points).

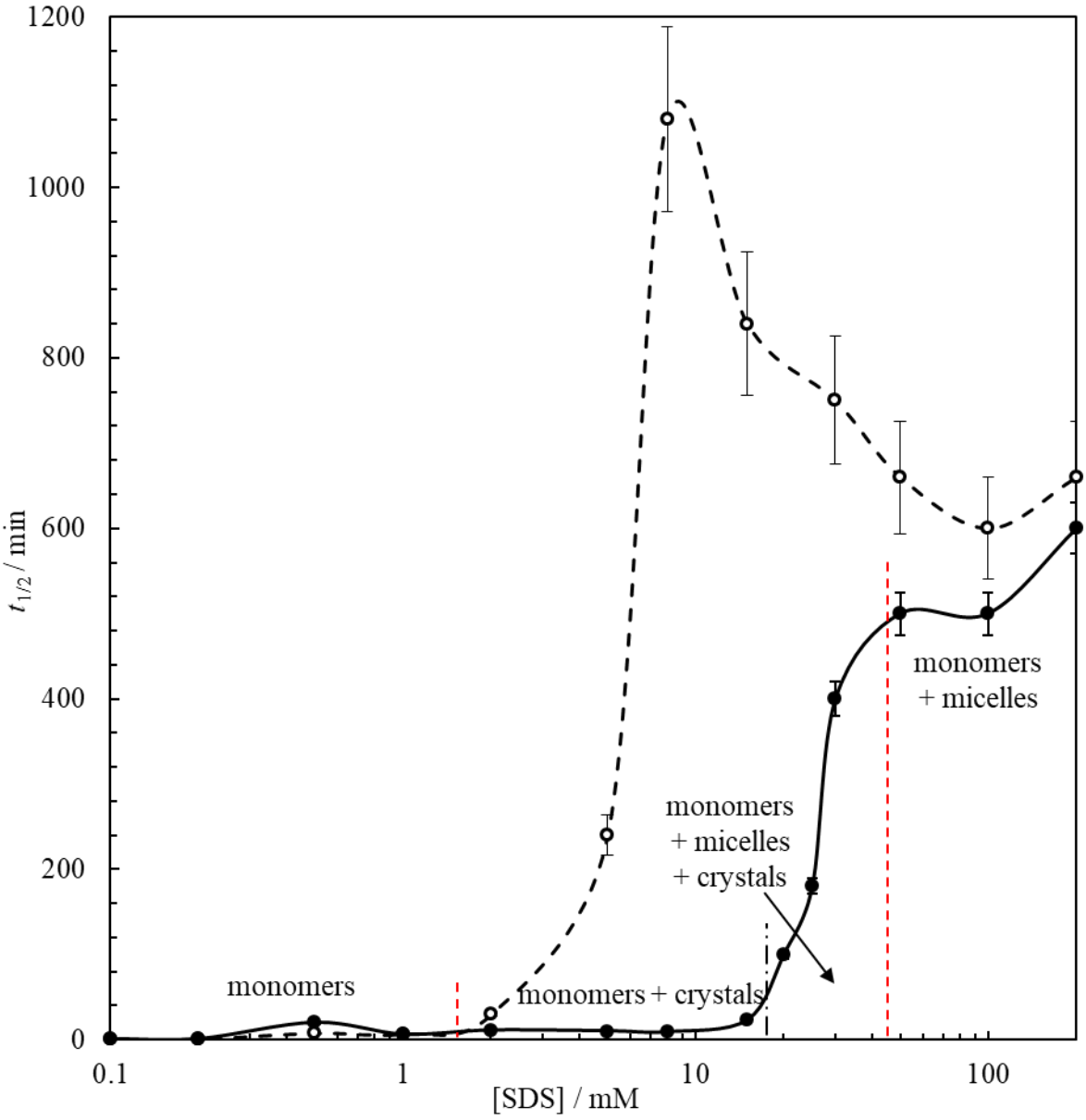

Figure 6. Microscope images of aqueous foams generated from 1 mM-100 mM SDS in 10 mM $Mg(NO_3)_2$ crystal dispersions at different surfactant concentrations (given).

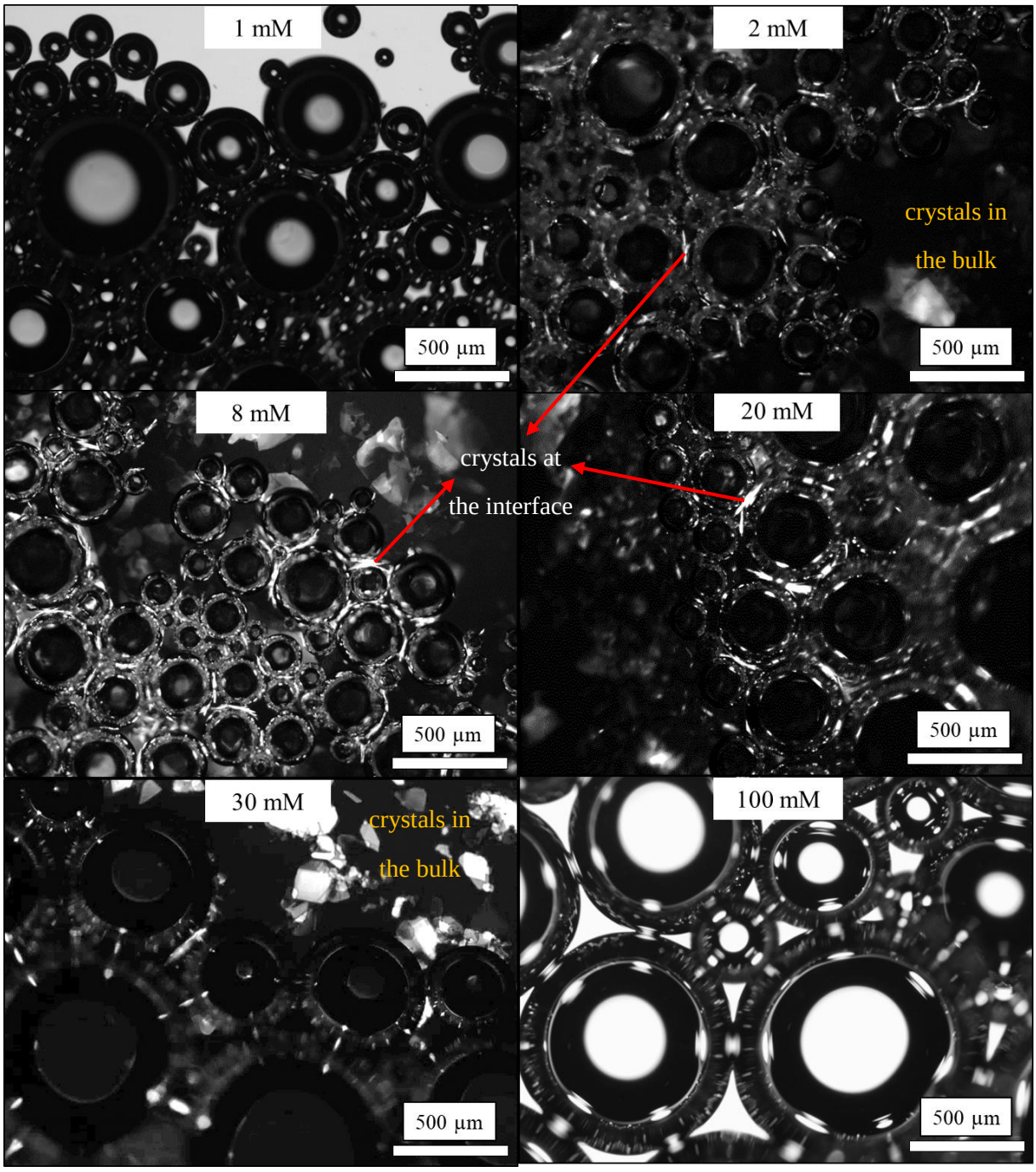

Figure 7. Microscope images of aqueous foams generated from 15 mM SDS in 1 mM-50 mM $Mg(NO_3)_2$ crystal dispersions at different salt concentrations (given).

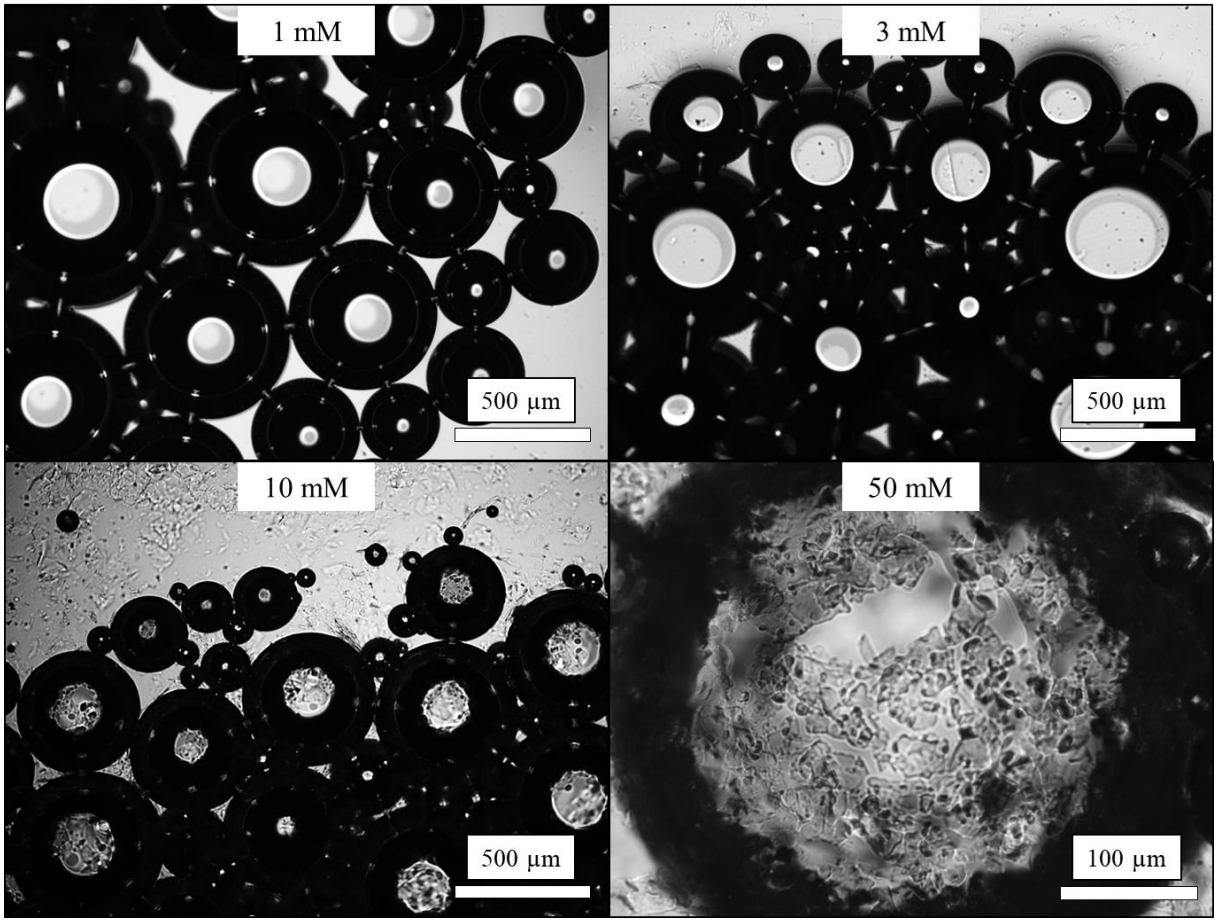

Figure 8. Variation of the ratio of foam volume after 2 days at 20 ± 3 °C to that just after preparation for 20 mL of (a) varying [SDS] in 10 mM $Mg(NO_3)_2$ and (b) varying $Mg(NO_3)_2$ in 15 mM SDS.

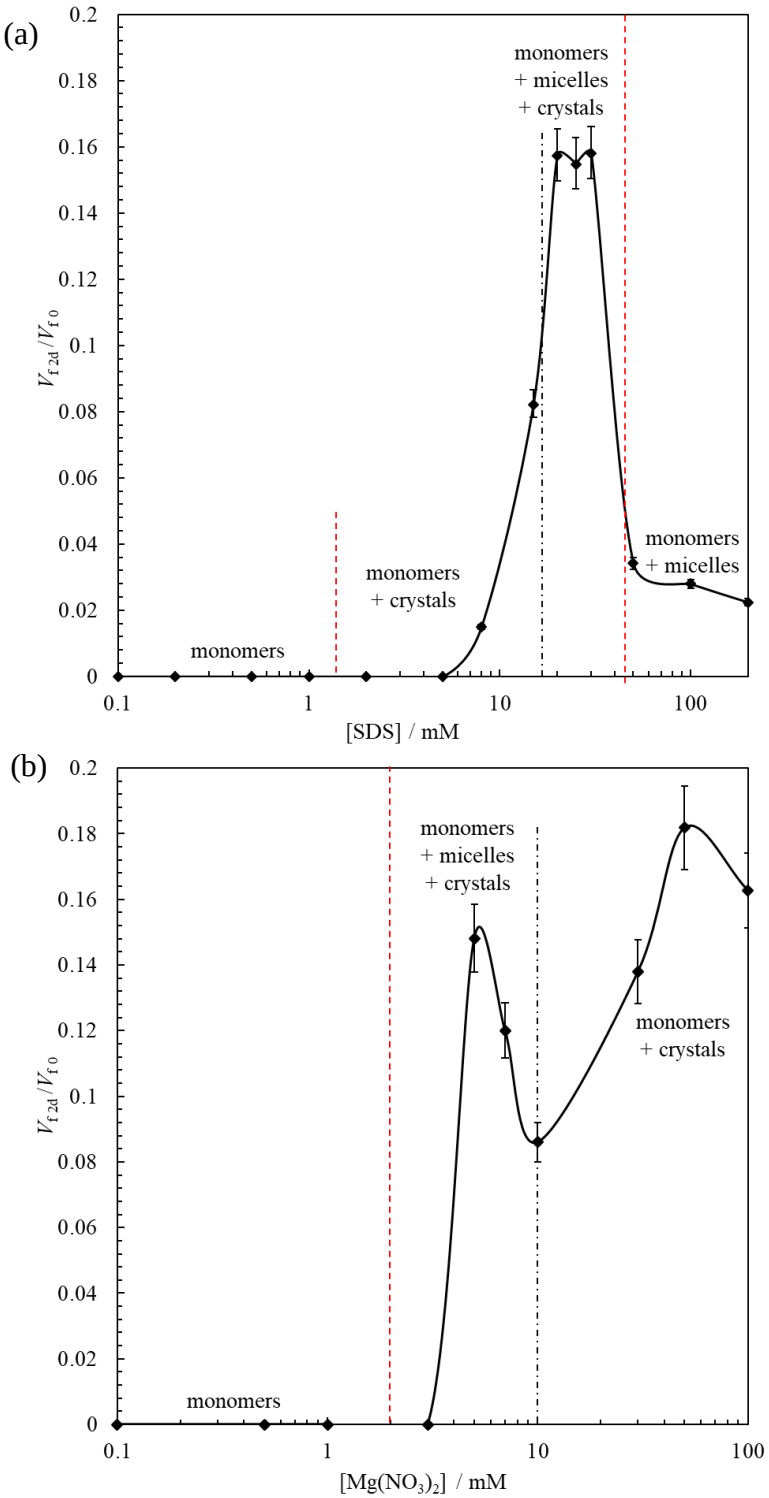

Figure 9. Variation of initial foam volume (V_{f0}) of 20 mL of supernatant, sediment or crystal dispersion as a function of actual SDS concentration. Supernatant and sediment were separated from crystal dispersions of various [SDS] in 10 mM $Mg(NO_3)_2$. For comparison, the variation of the calculated initial foam volume of crystal dispersions is plotted with a dashed line.

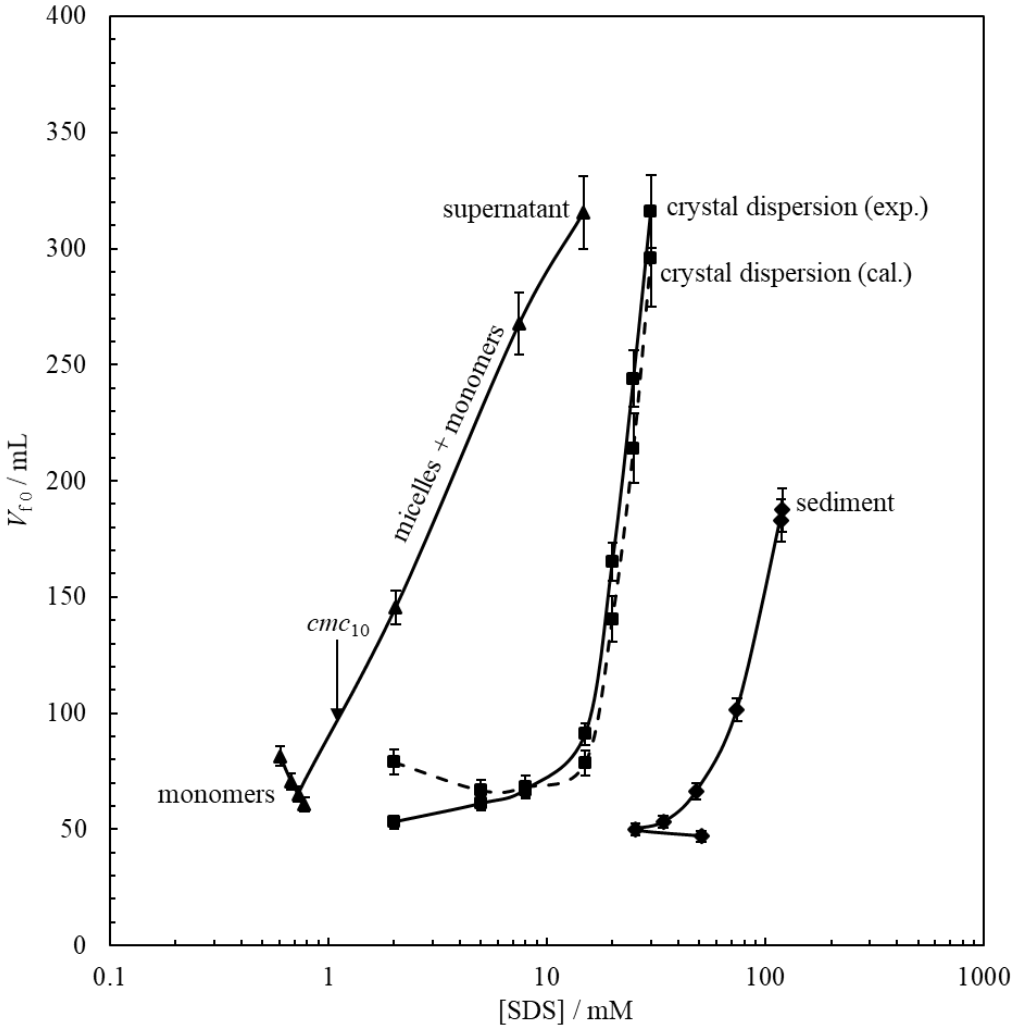

Figure 10. Variation of foam half-life ($t_{1/2}$) of 20 mL of supernatant, sediment and crystal dispersion as a function of actual SDS concentration. Supernatant and sediment were separated from crystal dispersions of various [SDS] in 10 mM $Mg(NO_3)_2$.

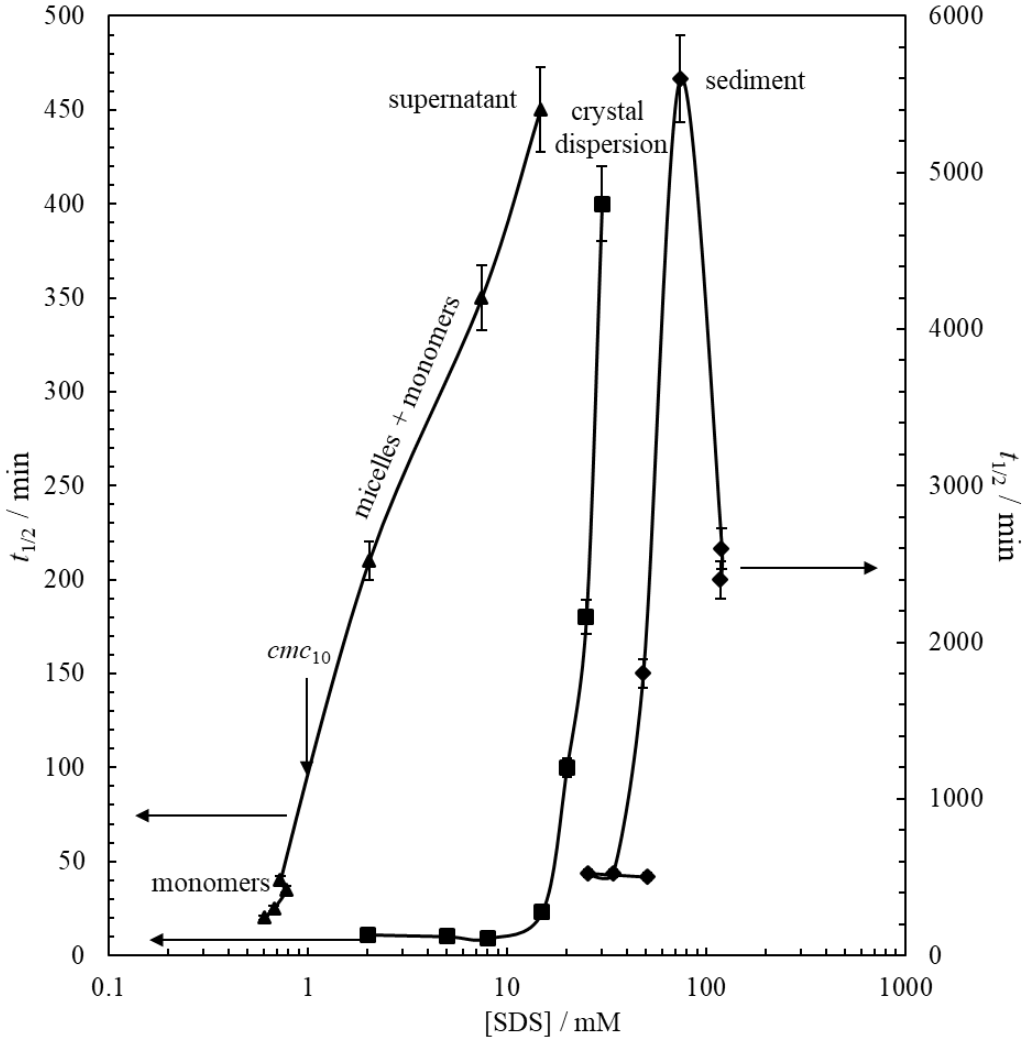

Figure 11. Cross-polarised microscope images of foams generated from (left) crystal dispersion of SDS in 10 mM $Mg(NO_3)_2$ at (a) 8 mM, (b) 20 mM and (c) 30 mM SDS and (right) corresponding sediment. Images were taken just after preparation. (d) Cryo-SEM images of (left) surfactant crystals sampled from a crystal dispersion of 20 mM SDS in 10 mM $Mg(NO_3)_2$ (white fibers are salt crystals) and (right) the surface of a bubble in a foam generated from the sediment separated from it.

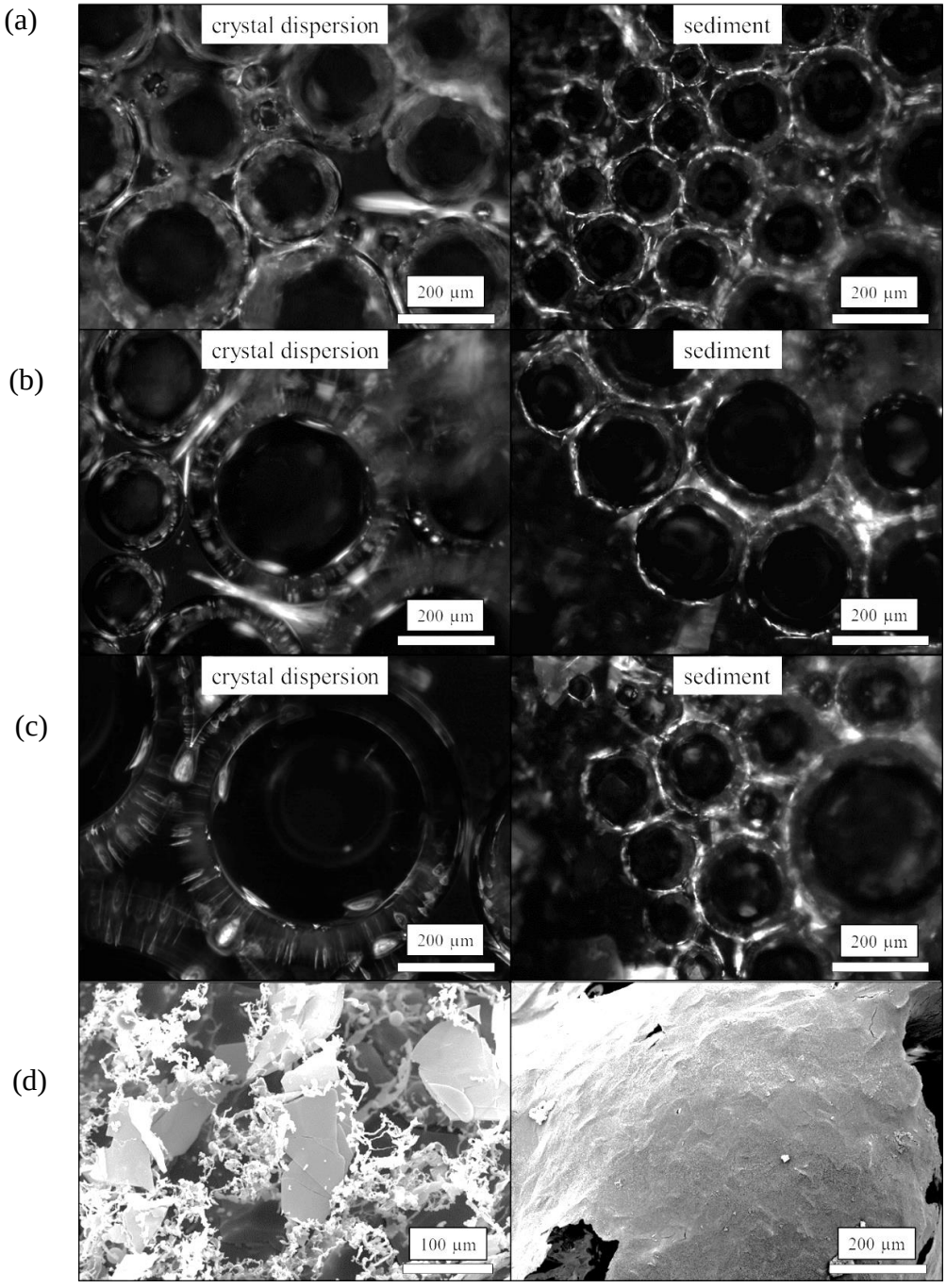

Figure 12. (a) Optical microscope images of crystal dispersions of 30 mM SDS in 10 mM $Mg(NO_3)_2$ after sonication for various times. (b) Variation of initial foam volume (V_{f0}) and foam half-life ($t_{1/2}$) of aqueous foams generated from 20 mL of ultrasound-treated crystal dispersions as a function of average crystal diameter (D). V_{f0} and $t_{1/2}$ values without sonication are denoted by dashed circles.

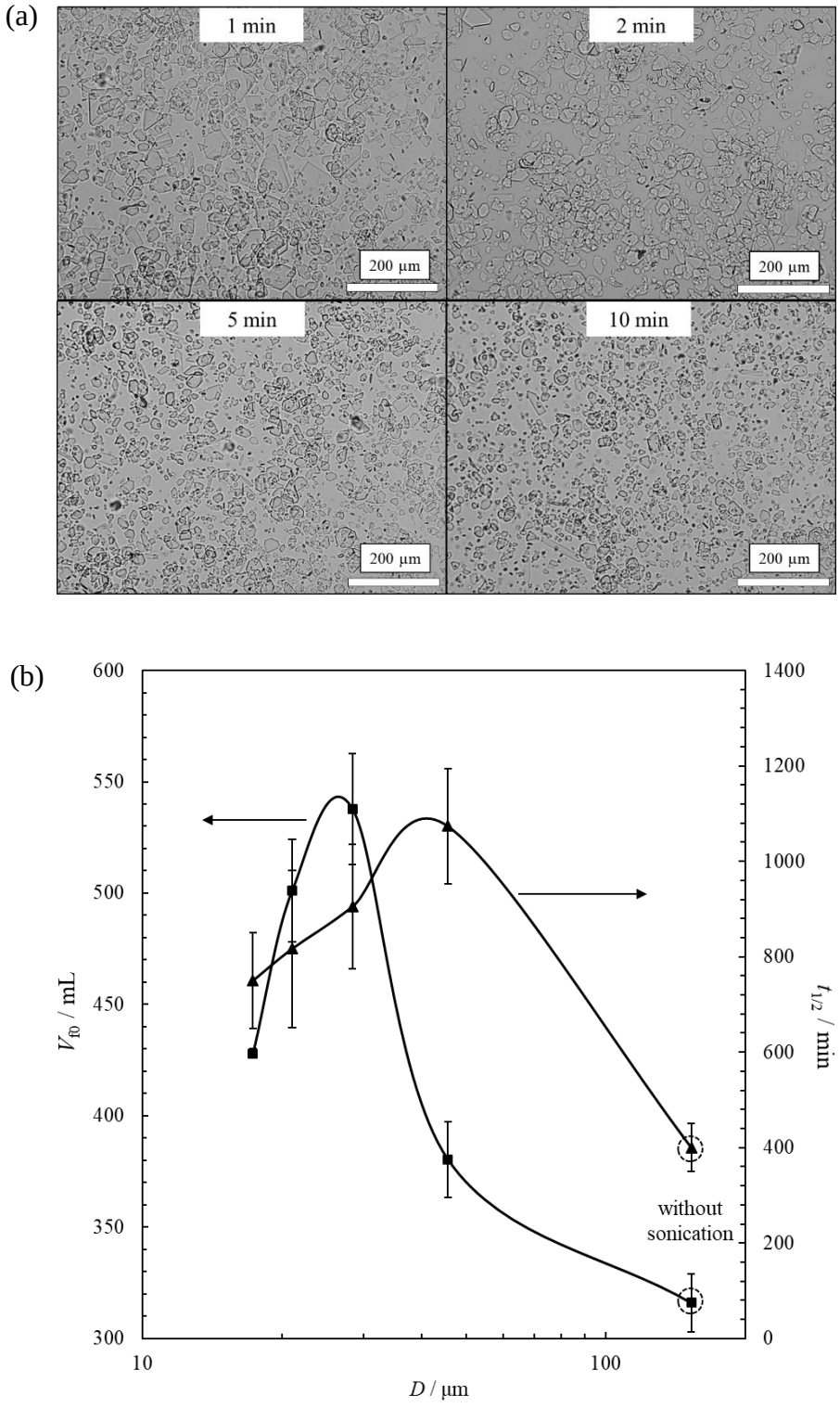

Figure 13. (a) Optical microscope images of crystal dispersions of SDS in 10 mM $Mg(NO_3)_2$ at various [SDS] prepared by rapid cooling. (b) Variation of initial foam volume (V_{f0}) and foam half-life ($t_{1/2}$) of aqueous foams generated from 20 mL of the crystal dispersions above as a function of [SDS] (filled points). Data for the same crystal dispersions prepared at room temperature are given as open points.